Journal of Sound and Vibration (1998) **218**(1), 133–157
Article No. sv981808

VEHICLE DRIVELINE DYNAMIC BEHAVIOUR: EXPERIMENTATION AND SIMULATION

PH. COUDERC, J. CALLENAERE, J. DER HAGOPIAN AND G. FERRARIS

Institut National des Sciences Appliquées de Lyon, *LMSt*, *Bâtiment* 113-20, *avenue Albert Einstein*, 69621, *Villeurbanne Cedex*, *France*

A. KASSAI, Y. BORJESSON, L. VERDILLON AND S. GAIMARD

RENAULT, *UET Tenue et Acoustique*, *DDT*, 250 *Route de l'Empereur*, 92562 *Rueil-Malmaison*, *France*

(*Received* 21 *November* 1997, *and in final form* 24 *June* 1998)

The work presented is of a study of torsional vibrations of a driveline under static torque and excited by engine torque fluctuations. It includes the design of an experimental set-up and a computer software to predict dynamic behaviour and seek efficient technical solutions. A finite element model is used to study current systems and perform transient analyses. Basic linear elements are used and non-linearities such as a multi-staged clutch with dry friction and gear backlash are taken into account. The time response is calculated and a pseudo-modal method is used. An experimental set-up of the whole driveline has been designed and built to allow simulation of the basic torsional phenomena occurring on the vehicle driveline under input torque from 0 to 200 Nm, and, moreover, to validate numerical models. Furthermore, prediction and experiments on two new vehicles are in quite good agreement.

1. INTRODUCTION

Increasing customer demands for quieter vehicles have resulted in the need for better understanding of the dynamic behaviour of drivelines and for the reduction of torsional vibrations to an acceptable level. This work is particularly focused on vehicle driveline torsional vibrations excited by engine torque fluctuations under an input torque from 0 to 200 Nm. This involves taking into account many types of excitation and non-linear effect in order to study transient phenomena. Thus, there is a need for suitable non-linear models leading to better understanding of torsional driveline dynamics and efficient and practical solutions for vehicle manufacturers.

Driveline torsional vibrations fall into two broad categories, namely gear rattle and driveline vibration. Gear rattle is classified as quasi-steady impulsive noise. The basic source is usually a component or sub-system with clearance non-linearities which includes backlashes, multi-valued stiffness characteristics, dry friction, hysteresis, etc. Driveline vibrations create noises emanating from the

0022–460X/98/460133 + 15 $30.00/0

driveline when loaded. The resonant driveline behaviour can amplify gear motion at certain engine speeds of rotation, thus requiring frequency analysis.

Most of the models used for the driveline torsional vibration analysis are lumped discrete models with a few degrees of freedom. The non-linear torsional characteristics of a clutch disc and the backlash of an input shaft and countershaft are taken into account and the investigators have focused on periodic vibro-impacts at the unloaded gear meshes/splines, with backlashes in manual transmissions [1–4]. These phenomena have been studied by using a variety of techniques, such as simulation [5–7], quasi-steady state analysis [8–10], the multi-body approach [11] and experimental noise perception [12, 13]. Time integration schemes are generally used to solve the governing equations and perform transient analysis. Most of these works deal with idle gear rattle in manual transmissions but certain ones are concerned with driveline vibrations. Theoretical and experimental investigations have established that several factors may have significant influence on the torsional dynamic behaviour of drivelines [5, 14–18]: inertia, multi-staged clutch disc, gearbox drag torque, dry friction and gear backlash.

Both experimental and theoretical research have been focused on the torsional vibrations of the complete driveline in controlling the natural frequencies and mode shapes of the system [17, 19, 20]. Also, analytical and experimental results have demonstrated that a system approach is necessary to understand torsional resonant phenomena occurring within certain ranges of operating speeds. Useful experimental research has been conducted to analyze these phenomena with emphasis placed on the analysis of driveline resonance. In addition, the authors have investigated the source of drive rattle either by instrumenting test vehicles [5, 6, 14], and by conducting tests on torsionally excited experimental set-ups composed of the flywheel, the clutch disc and the transmission in neutral position [10, 15, 21].

The aim of the work described in this paper is a part of that of reference [18] and concerns the prediction of the dynamic behaviour of vehicle drivelines, showing good agreement between simulation and experimental results. First, the description of the driveline and the torsional phenomena are presented. Then, a torsional finite element model including gear backlash and a multi-staged non-linear clutch with dry friction is used to study the dynamic behaviour of current systems and to perform transient analysis. This part deals with the numerical method associated with a pseudo-modal method to solve the differential equations governing the motion. It also presents the computer simulation approach that has successfully satisfied the above demands for a research and design tool for prediction of dynamic behaviour. The third part deals with the experimental study. An experimental set-up of a vehicle driveline has been designed and built. It allows simulation of the basic phenomena occurring in vehicles, when torque is applied, and validation of the numerical models. Software including the signal processing of instantaneous rotational speed has been developed for analyzing experimental results. Finally, the time responses calculated are validated on two new vehicles by comparing numerical and experimental results.

2. DESCRIPTION OF DRIVELINE AND TORSIONAL PHENOMENA

2.1. DESCRIPTION OF DRIVELINE

A vehicle driveline is composed of many components transmitting engine mechanical energy to the wheels. It links the engine to the wheels and ensures gear reduction for the use of the engine in its optimum operating range. A classical front-engine front-wheel-drive vehicle is illustrated in Figure 1 and the following components are identified.

The first is the flywheel whose inertia reduces the magnitude of angular accelerations generated by engine torque irregularities.

The second is the clutch assembly which is composed of the clutch disc and the clutch mechanism. Its main functions are to connect and disconnect the gearbox with the engine, to progressively transmit engine torque to the input shaft, and to provide vibratory isolation from engine torque fluctuations. This function is achieved by two systems rotationally linked by an elastic and dissipative system which can rotate together (see Figure 2). The first system is the clutch disc and rings connected to the flywheel, and the second is the clutch hub connected to the input shaft via spline backlash. The mean torque is transmitted through a set of preloaded springs.

The third is the gearbox which includes a large number of couples of helical gears for gear reduction, and a differential to distribute torque to the wheels. In current gearboxes, unloaded driven gears are generally assembled on the

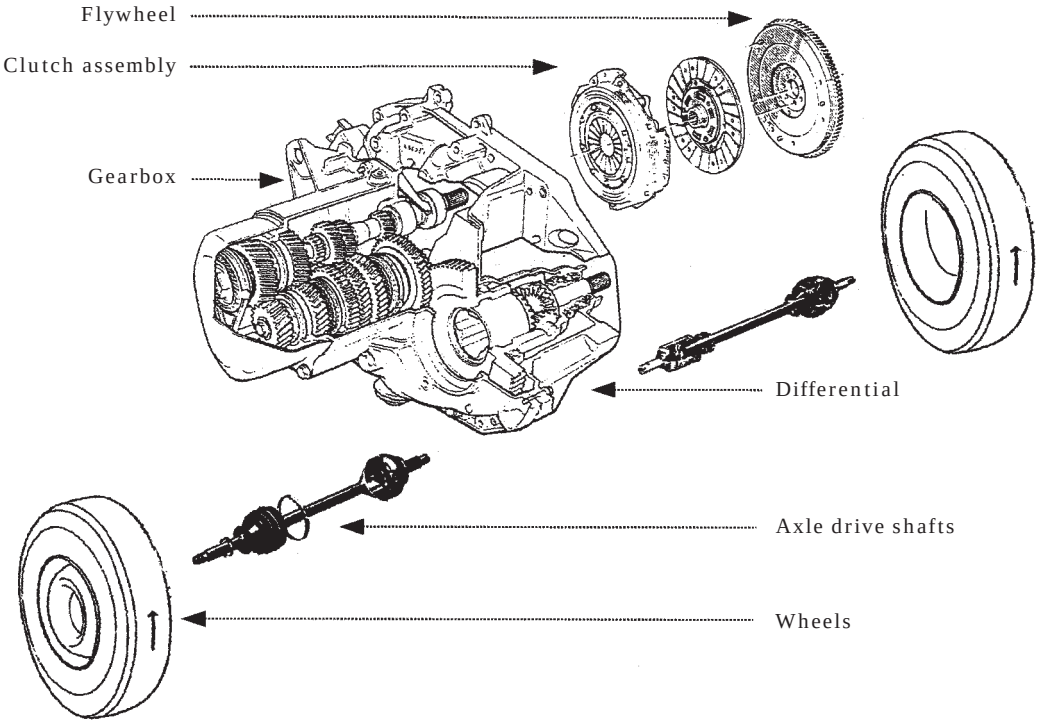

Figure 1. Front-engine front-wheel-drive vehicle driveline.

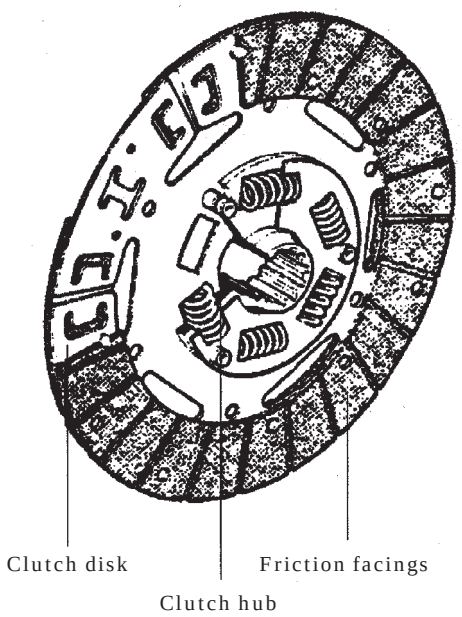

Figure 2. Clutch plate.

countershaft. They are in continuous meshing contact with the drive gears of the input shaft. When the clutch is engaged, the driven gear is connected to the countershaft after speed synchronization and claw coupling. The gearbox used in this study is shown in Figure 3. It is composed of four shafts: the input shaft where

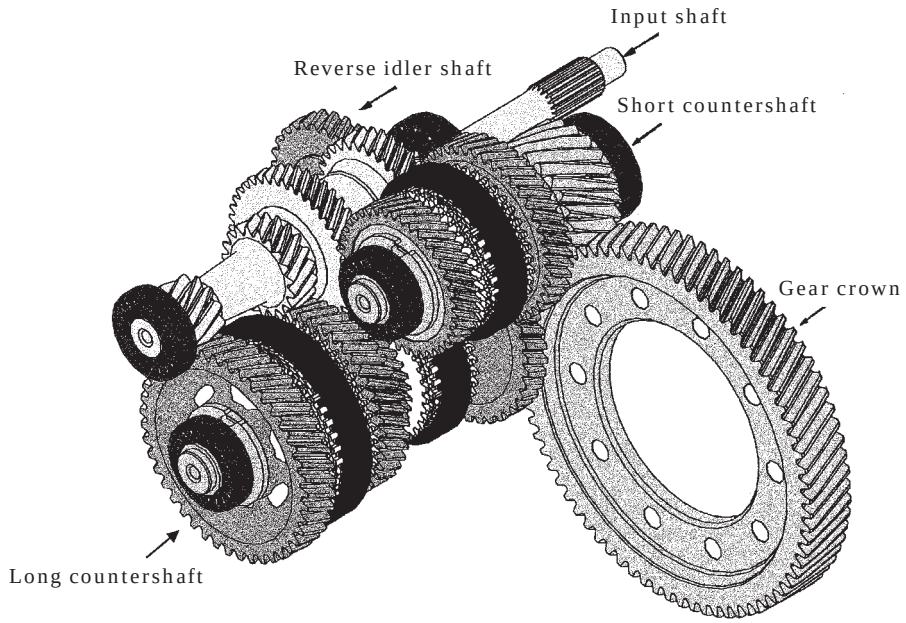

Figure 3. Five-speed manual transmission of the Renault Safrane vehicle.

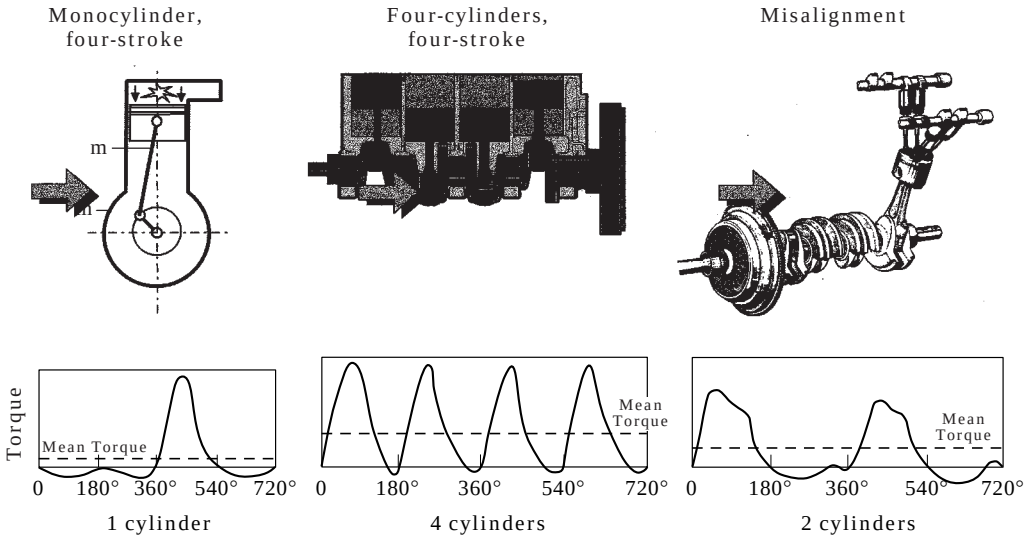

Figure 4. Engine torque fluctuations.

drive pinions are solid, a long countershaft with the idle pinions of the first, second, fifth and reverse gears, a short countershaft with the idle pinions of the third and fourth gears and the reverse idler shaft. Unloaded gears are the major source of gear rattle because of the vibro-impacts caused by engine torque fluctuations.

The fourth and fifth are the two drive axle shafts that transmit the engine torque from the differential to the wheels. They are generally composed of two homokinetic joints and a shaft. In the case of a transverse engine vehicle whose gearbox is not in the center line, the two drive axle shafts have different lengths and an intermediate shaft is necessary.

2.2. SOURCE OF TORSIONAL VIBRATION

Engine torque fluctuations involve engine angular accelerations which are the major cause of driveline torsional vibrations. These torque fluctuations are the sum of discrete torque pulses due to combustion pressure in the cylinders and cyclic inertia torques due to reciprocating pistons. In a four-cylinder four-stroke engine, the flywheel angular velocity is synchronized with the engine combustion which fluctuates repeatedly at a firing pulse frequency of twice per engine revolution. Thus, the dynamic torque is the sum of a constant mean torque and an oscillating torque whose frequency spectrum is essentially composed of the even harmonics, which are preponderant for a four-cylinder engine (see Figure 4). Misalignment between the transmission input shaft, clutch disc and crankshaft axis of rotation can generate excitation forces synchronous with the engine speed of rotation. The high inertia of the engine flywheel tends to reduce the magnitude of angular accelerations which are particularly high at idle speed and in diesel engines. Unfortunately, it also reduces the acceleration of the vehicle, resulting in sluggish performance.

2.3. TORSIONAL PHENOMENA

The following torsional phenomena occurring on the vehicle driveline are concerned in this work.

2.3.1. *Idle gear rattle*

At idle speed, the transmission is in neutral position and the clutch is engaged. Engine torque fluctuations cause collisions between gears and/or spline teeth in the gearbox and the clutch hub. Since backlashes actually exist in all geared systems and, in neutral, all gear and spline meshes are essentially unloaded, thus they are all potential rattle sources.

2.3.2. *Drive rattle*

Drive rattle and idle gear rattle are similar; however, resonance frequencies of the driveline can affect the nature of drive rattle. Drive rattle is a phenomenon caused mainly by the non-linear torsional vibration of the driveline. This causes collision between the gear teeth in the transmission which in turn causes excitation forces, making the bearings of the gearbox vibrate. A conventional clutch damper can greatly reduce the drive rattle.

2.3.3. *Surging*

Surging results from sudden changes of engine torque actuating the driveline. The first mode shape is involved and the vehicle is subjected to damped rocking motion. This phenomenon occurs during sharp accelerations at low engine speed and results from a tip-in or back-out procedure.

2.3.4. *Booming noise and hammering*

Booming noise involves a mode shape concerning transmission drive axle shafts, and hammering is essentially generated by tripod joints.

3. TORSIONAL MODEL

Since there are a number of driveline configurations resulting from in-line and transverse engines, front and rear wheel drive, direct and indirect gearboxes etc., computer software is required to analyze a specific driveline configuration and a lumper parameter approach is used. The driveline is represented as a chain of torsional simple branched systems describing the various components and the model chosen includes linear basic elements and three non-linearities arising from clearances, non-linear stiffness, and clutch dry friction effects. The representation of the torsional model the driveline is shown in Figure 5. It allows a linear modelling approach in analyzing the natural frequencies, the mode shapes and the steady state behaviour of the driveline, and in analyzing of the transient phenomena generated by the non-linearities.

3.1. COMPONENT MODELLING

A typical model for a front-engine front-wheel-drive vehicle is composed of the driveline, the vehicle chassis and the Motive Power Unit (MPU). The model of the driveline can be divided into the following different sub-systems: flywheel, clutch hub, front wheels and tires, axle drive shafts and homokinetic joints, all of which are modelled by using inertia, stiffnesses and viscous damping elements. A non-linear clutch element is introduced and a refined model is used for modelling the gearbox.

In addition to the above torsional model of the driveline, the three following translational degrees of freedom are introduced: longitudinal displacement of the right and the left front chassis and of the sub-system {vehicle chassis, MPU, rear chassis} considered as a rigid body. The contact between tires and road involves both the tire's torsional stiffness and the longitudinal stiffness linking the rear chassis to the vehicle chassis. This permits linking the angular rotation of the wheels to the vehicle's translational motion. The wheels are assumed to be connected to the ground: i.e., the effect of tire slip is neglected.

Basic linear discrete elements are used. These are simple inertia, torsional stiffness elements, viscous damper, connection elements representing a gear pair connected by a viscous damper and tooth stiffness, and one rod element with a circular cross-section. In addition, a special element for modelling the differential and two non-linear elements is developed comprising a multi-staged clutch with dry friction and gear backlash.

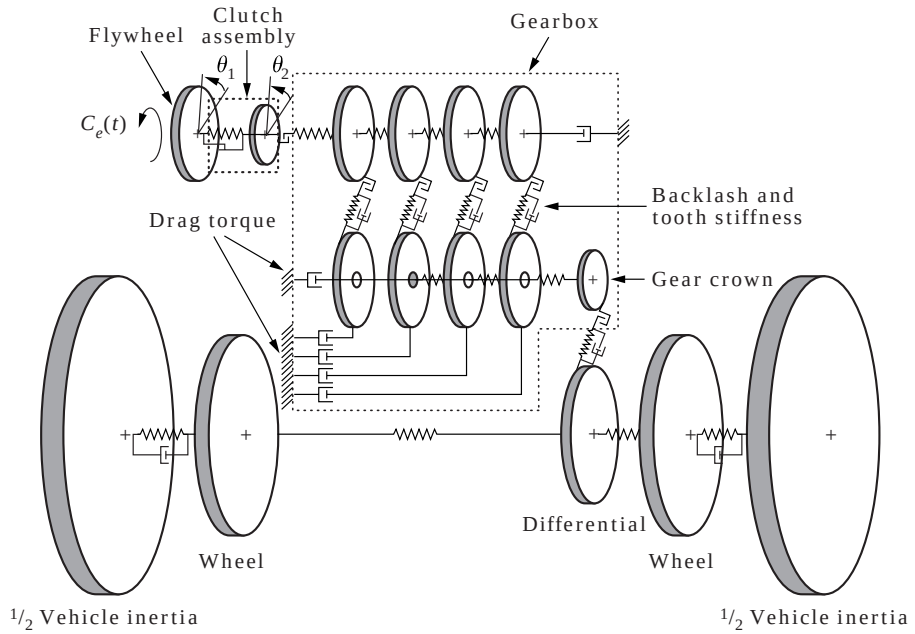

Figure 5. Torsional model of the whole driveline.

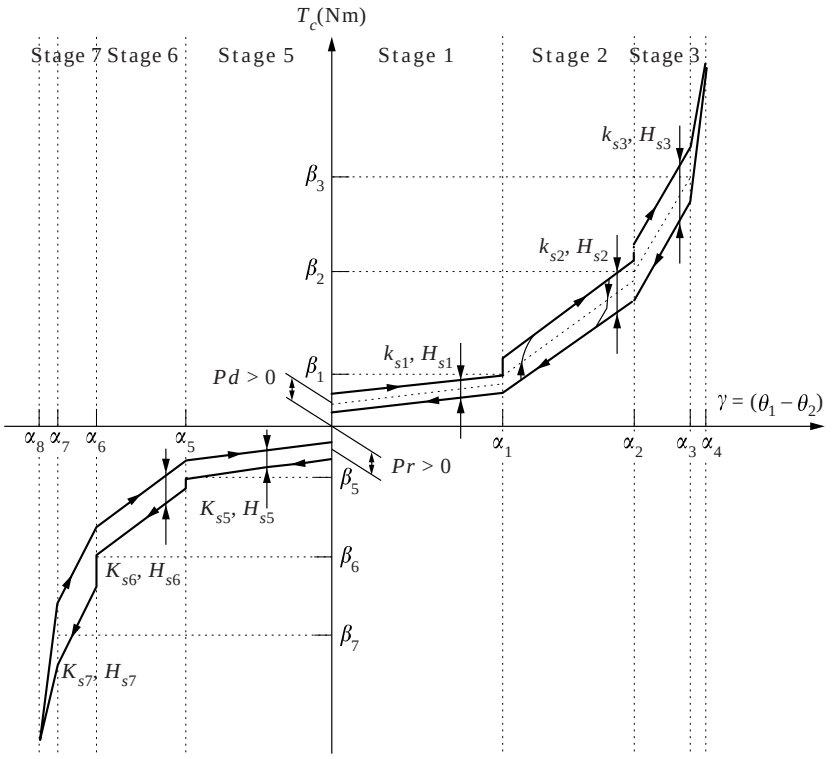

Figure 6. Non-linear dynamic characteristics of the clutch.

3.1.1. *Multistage clutch model*

The non-linear characteristics of the clutch, shown in Figure 6, are expressed as the clutch torque T_c, a function of γ, the relative angular displacement between the flywheel θ_1 and the clutch hub θ_2 (see Figure 5). These non-linearities can be introduced by T_c as a piece-wise linear function described by (a list of symbols is given in the Appendix)

$$T_c = k_{si}(\theta_1 - \theta_2 - \alpha_i) + \beta_i + (H_{si}/\pi) \arctan [\sigma(\dot{\theta}_1 - \dot{\theta}_2)]. \tag{1}$$

The hysteresis is modelled by a Coulomb friction law. In this case, the damping force is constant and the sign depends on the direction of the relative rotation. For each stage, the angular range α_i, the stiffness k_{si}, and the hysteresis $H_{si}/2$ are taken into account and two preloaded torques (P_d and P_r; see Figure 6) can be introduced.

The function $(H_{si}/\pi) \arctan [\sigma(\dot{\theta}_1 - \dot{\theta}_2)]$ (see Figure 7) smooths the effects of dry damping on the clutch when the torque climbs from a negative to a positive value, or on the contrary, thus leading to numerical stability in simulations.

The clutch mass matrix is classical and its stiffness matrix $[K_c]$, viscous damping matrix $[C_c]$ and external torque excitation vector $[\mathbf{C}_{ext}]$ take the forms

$$[K_c] = \begin{bmatrix} k_{si} & -k_{si} \\ -k_{si} & k_{si} \end{bmatrix}, \qquad [C_c] = \begin{bmatrix} c_c & -c_c \\ -c_c & c_c \end{bmatrix},$$

$$[\mathbf{C}_{ext}] = \begin{bmatrix} T_{eng}(t) + k_{si}\alpha_i - \beta_i - (H_{si}/\pi) \arctan(\sigma(\dot{\theta}_1 - \dot{\theta}_2)) \\ -k_{si}\alpha_i + \beta_i + (H_{si}/\pi) \arctan(\sigma(\dot{\theta}_1 - \dot{\theta}_2)) \end{bmatrix}. \tag{2}$$

The matrix $[K_c]$ depends on the state γ of the clutch, whereas the excitation vector $[\mathbf{C}_{ext}]$ depends on the torque $T_{eng}(t)$ applied by the motor drive and the state γ of the clutch.

3.1.2. *Gear backlash model*

The gear backlash is included by a non-linear mesh function restricting the displacement of a floating part corresponding to a gap. The model used is shown in Figure 8. When the teeth are separated, the force is zero. Non-zero force is characterized by linear stiffness and viscous damping. The gap situation is based on the relative linear translational pitch line displacement δ of two meshing gears. The non-linear function T_g described in the following equations depends on the physical system while the symmetric clearance-type function $y(\delta, b_g)$ gives both single-sided impacts and double-sided impacts:

$$T_g = -k_g R y(\delta, b_g) - c_g R \dot{y}(\delta, b_g), \tag{3}$$

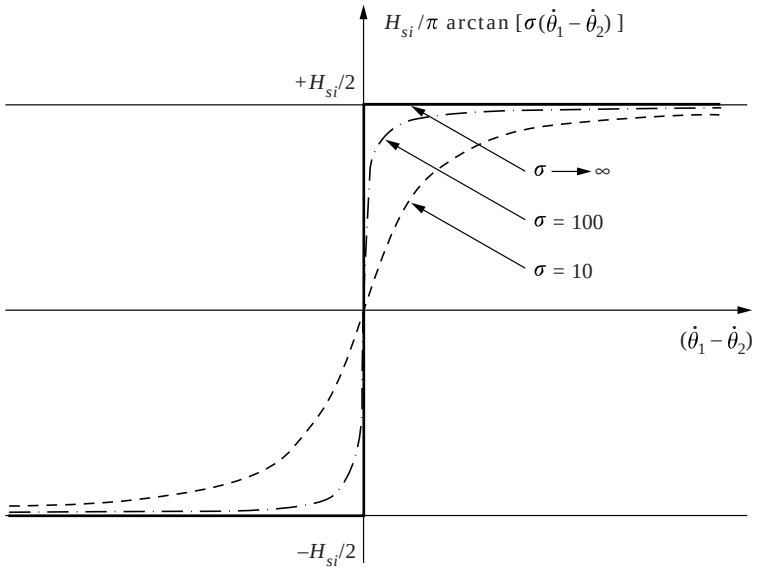

Figure 7. Plot of the function $(H_{si}/\pi) \arctan[\sigma(\dot{\theta}_1 - \dot{\theta}_2)]$. ——, $\sigma \to \infty$; –·–·–, $\sigma = 100$; – – –, $\sigma = 10$.

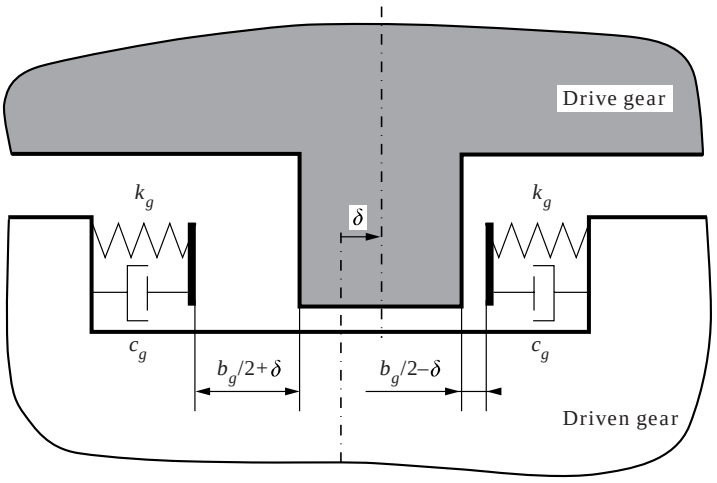

Figure 8. Model of gear backlash.

with

$$y(\delta, b_g) = \begin{Bmatrix} (\delta - b_g/2), & \delta \geqslant b_g/2 \\ 0, & -b_g/2 < \delta < b_g/2 \\ (\delta + b_g/2), & \delta \leqslant -b_g/2 \end{Bmatrix}, \tag{4}$$

and

$$\dot{y}(\delta, b_g) = \begin{Bmatrix} \dot{\delta}, & \delta \geqslant b_g/2 \\ 0, & -b_g/2 < \delta < b_g/2 \\ \dot{\delta}, & \delta \leqslant -b_g/2 \end{Bmatrix}. \tag{5}$$

The stiffness and damping matrices, $[K_{gi}]$ and $[C_{gi}]$, of the gear i can be written as

$$[K_{gi}] = \begin{bmatrix} k_g R_{pi}^2 & k_g R_{pi} R_{qi} \\ k_g R_{pi} R_{qi} & k_{gi} R_{qi}^2 \end{bmatrix}, \qquad [C_{gi}] = \begin{bmatrix} c_g R_{pi}^2 & c_g R_{pi} R_{qi} \\ c_g R_{pi} R_{qi} & c_g R_{qi}^2 \end{bmatrix} \tag{6}$$

when the teeth of the drive gear are in contact with those of the driven gear. $[K_{gi}]$ and $[C_{gi}]$ are nil in the other case.

3.1.3. *Sub-system {vehicle chassis, MPU, rear chassis, rear transmission}*

The model (Figure 9) includes the driveline rotational degree of freedom and the three displacement degrees of freedom. The modal displacement vector $\boldsymbol{\delta}_{ss}$ takes the form

$$\boldsymbol{\delta}_{ss} = \{\theta_{fl}, \theta_{fr}, X, X_{fl}, X_{fr}\}. \tag{7}$$

The kinetic energy T and the strain energy U of the translational sub-system can be written as

$$T = \tfrac{1}{2}(I_{fl}\dot{\theta}_{fl}^2 + I_{fr}\dot{\theta}_{fr}^2 + M_v\dot{X}^2 + M_{fl}\dot{X}_{fl}^2 + M_{fr}\dot{X}_{fr}^2), \tag{8}$$

$$U = \frac{1}{2}\left[\frac{K_t}{R^2}((X_{fl} + R\theta_{fl})^2 + (X_{fr} + R\theta_{fr})^2) + K_{lfc}(X - X_{fl})^2 + K_{rfc}(X - X_{fr})^2\right]. \tag{9}$$

Applying the Lagrange equations yields the mass and the stiffness matrices $[M_{ss}]$ and $[K_{ss}]$ as

$$[M_{ss}] = \begin{bmatrix} I_{fr} & 0 & 0 & 0 & 0 \\ 0 & I_{fl} & 0 & 0 & 0 \\ 0 & 0 & M_v & 0 & 0 \\ 0 & 0 & 0 & M_{fl} & 0 \\ 0 & 0 & 0 & 0 & M_{fr} \end{bmatrix},$$

$$[K_{ss}] = \begin{bmatrix} K_t & 0 & 0 & K_t/R & 0 \\ 0 & K_t & 0 & 0 & K_t/R \\ 0 & 0 & K_{rfc} + K_{lfc} & -K_{lfc} & -K_{rfc} \\ K_t/R & 0 & -K_{lfc} & K_t/R^2 + K_{lfc} & 0 \\ 0 & K_t/R & -K_{rfc} & 0 & K_t/R^2 + K_{rfc} \end{bmatrix}. \tag{10}$$

3.1.4. *Governing equations*

Differential equations governing the motion of the complete system are derived from the Lagrange equations and are written as

$$[M] \cdot \{\ddot{\boldsymbol{\delta}}\} + [C(\delta, \gamma)] \cdot \{\dot{\boldsymbol{\delta}}\} + [K(\delta, \gamma)] \cdot \{\boldsymbol{\delta}\} = \{\mathbf{C}_{ext}(\delta, \gamma)\}, \tag{11}$$

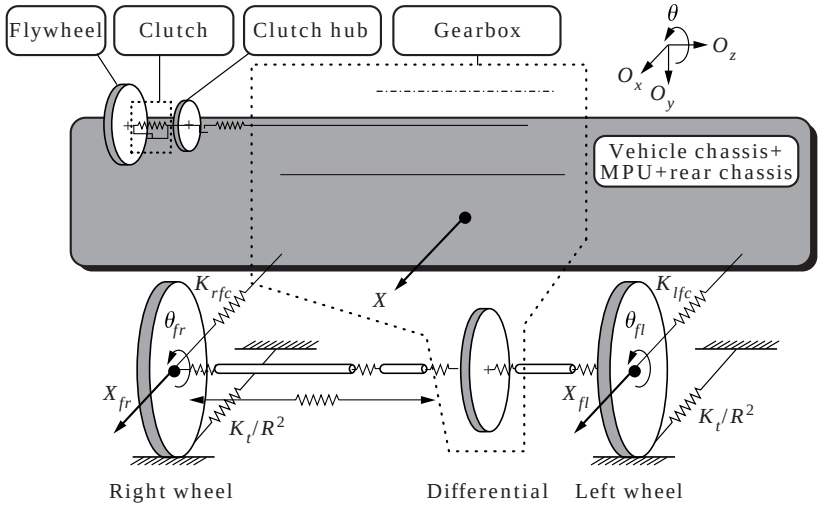

Figure 9. Diagram of the {driveline, box body and MPU} model.

where $[M]$ is the classical mass matrix $[K(\delta, \gamma)]$ is the non-linear stiffness matrix including matrices of classical elements, the clutch element $[K_c]$, and the gear pair elements $[K_{gi}]$. $[C(\delta, \gamma)]$ is the non-linear damping including the classical damping elements, the clutch element $[C_c]$ and the gear pair elements $[C_{gi}]$. $\{\mathbf{C}_{ext}(\delta, \gamma)\}$ is the exciting force vector including a part of the non-linear behavior of the clutch, while $\{\boldsymbol{\delta}\}$, $\{\dot{\boldsymbol{\delta}}\}$ and $\{\ddot{\boldsymbol{\delta}}\}$ are respectively the displacement, velocity and acceleration vectors.

One can notice that $[K(\delta, \gamma)]$, $[C(\delta, \gamma)]$ and $\{C_{ext}(\delta, \gamma)\}$ depend on the two non-linearity indicators and are up-dated at each step for the time response.

3.1.5. *Pseudo-modal method and numerical integration*

After defining the driveline model, inertia, stiffness and viscous matrices are automatically assembled by the computer program. These matrices, defined under several stages of the clutch, with or without contact between the teeth of the gears, lead to the determination of modal bases. For each case, the natural frequencies and mode shapes of the driveline are deduced from

$$[K(\delta, \gamma) - \omega^2 M]\{\Delta\} = \{0\}. \tag{12}$$

The pseudo-modal method has been used to introduce modal damping in the equations and to reduce considerably the dimension of the system [22]. The modal basis is composed of the n lowest mode shapes used in the equation

$$\{\boldsymbol{\delta}\} = |\phi|\{\mathbf{q}\}, \tag{13}$$

where $\{\boldsymbol{\delta}\}$ is the displacement vector, $\{\mathbf{q}\}$ the new set of co-ordinates and $|\phi|$ the modal basis. Equation (11) after premultiplication by $|\phi|^t$ gives

$$|\phi|^t[M]|\phi|\{\ddot{\mathbf{q}}\} + |\phi|^t[C(\delta, \gamma)]|\phi|\{\dot{\mathbf{q}}\} + |\phi|^t[K(\delta, \gamma)]|\phi|\{\mathbf{q}\} = |\phi|^t\{\mathbf{C}_{ext}(\delta, \gamma)\}. \tag{14}$$

Then modal damping values α_i, known from experiments or experience, are added on to the diagonal of matrix $|\phi|^t[C]|\phi|$. The time response is obtained by using a Newmark method applied at the modal basis of the drive line fitted to the right situation (stage of the clutch, contact or not between teeth gears).

3.2. COMPUTER SOFTWARE

The computer simulation software (25 000 lines) was developed by using MATLAB. First, the linkage between all the elementary matrices is performed and the mass, stiffness, and viscous damping matrices are built up. After computation of the modal basis, the simulation of the driveline dynamic behaviour is performed, enabling different kinds of analysis. Modal and forced vibration analyses are carried out to identify natural frequencies and mode shapes, as well as the frequency response of the linearized system. Transient time responses are also available, thereby introducing different types of torque derived from experimental data in the time domain.

4. EXPERIMENTAL STUDY

An experimental set-up has been designed and built to identify torsional phenomena occurring on a vehicle driveline and validate numerical models.

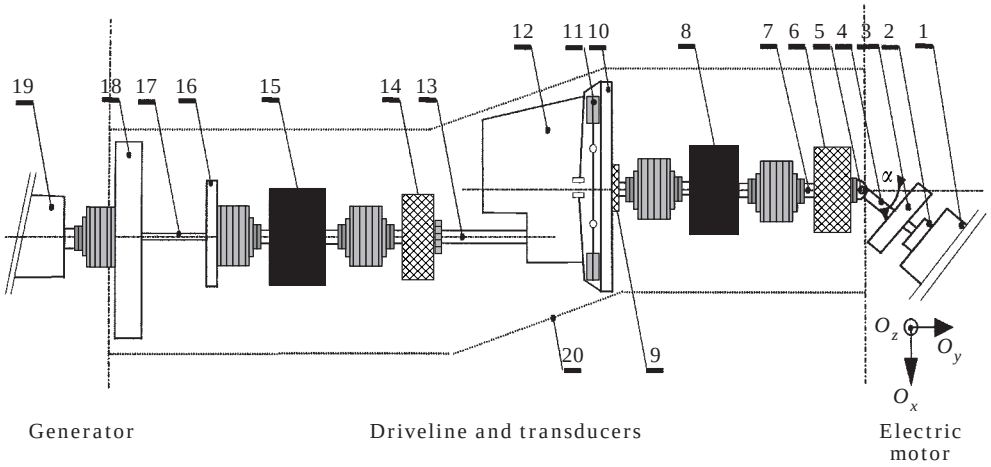

Figure 10. Diagram of the experimental set-up.

4.1. DESCRIPTION OF THE EXPERIMENTAL SET-UP

The experimental set-up shown in Figure 10 is composed of three parts: the driveline equipped with transducers, and two electromechanical devices. The first of these is a rotatory torsional exciter, which drives the driveline and introduces engine torque fluctuations at twice the engine speed of rotation, within a speed range from 0 to 3000 r.p.m. The second is a controlled system producing a resistive torque proportional to the drive torque for energy dissipation. The maximum values of torque and engine speed of rotation are, respectively, 3000 r.p.m. and 200 Nm at input, and 800 r.p.m. and 600 Nm at output.

4.1.1. *Mechanical assembly and motorization*

The driveline is composed of the flywheel (10), the clutch (11), the transmission with planet wheels locked (12), a drive axle shaft (13) equipped with a toothed wheel and an inertia corresponding to the front wheel (16). The supporting frame (20) receives mounts, driveline components and measurement devices while torquemeters are inserted between two torsional rigid couplings upstream (8) and downstream from (15) the gearbox. A low-pass mechanical filter is composed of a low stiffness torsional shaft (17), associated with a high value inertia (18). This experimental set-up has a mass of 6 tons, dimensions of 6×1 m and rests, damped by elastomer mounts, on a frame.

The rotatory torsional exciter is composed of a speed controlled 36-kW DC electric motor (1), and a maximum nominal torque value of 230 Nm is provided up to 1490 r.p.m. and then, with constant power up to 4000 r.p.m. A single Hooke's joint (5) is used to connect motor to the transmission input (4). A torque limiter (2) and a high value inertia (3) are also installed. A maximum angular value α of 16° between the axes of the two shafts is available. When the input shaft (4) is driven at constant speed, the angular velocity of the output shaft (7) varies periodically. Then the torque generated is the addition of a mean torque and an oscillating torque. The main harmonic of the output shaft torque is at twice the

input speed of rotation. The magnitude of the periodic torque increases as the angle α increases.

The resistive system is composed of a 113-kW generator (17) with a positive or negative torque controlled within a range from 0 to 800 Nm up to 1220 r.p.m. The low-pass mechanical filter allows the driveline to be vibration isolated from the generator. The control of the electric motor and generator is ensured by a PC equipped with ADC/DAC boards, using a specific control software. Figure 11 illustrates the experimental set-up. Figure 12 shows the transmission instrumented for measurements of gear motion and casing vibration.

4.1.2. *Instrumentation*

Torquemeters are inserted through the driveline upstream and downstream of the gearbox to measure static and dynamic torque and instantaneous velocity. The angular velocity of all the gears in the transmission are measured by using inductive probes targeted at the gear teeth and sensitive to magnetic flux fluctuations generated by teeth meshing. When torsional vibration occurs, the frequency of the alternating velocity components modulates the basic tooth form harmonic signal. An accelerometer is attached to the transmission casing to measure vibrations due to rattling gears. In addition, the temperature of the lubricant is controlled and regulated during testing.

4.1.3. *Data acquisition, measurements and signal processing*

All data are conditioned and simultaneously recorded by using an HP PARAGON acquisition system controlled by an HP700 computer. Storage and

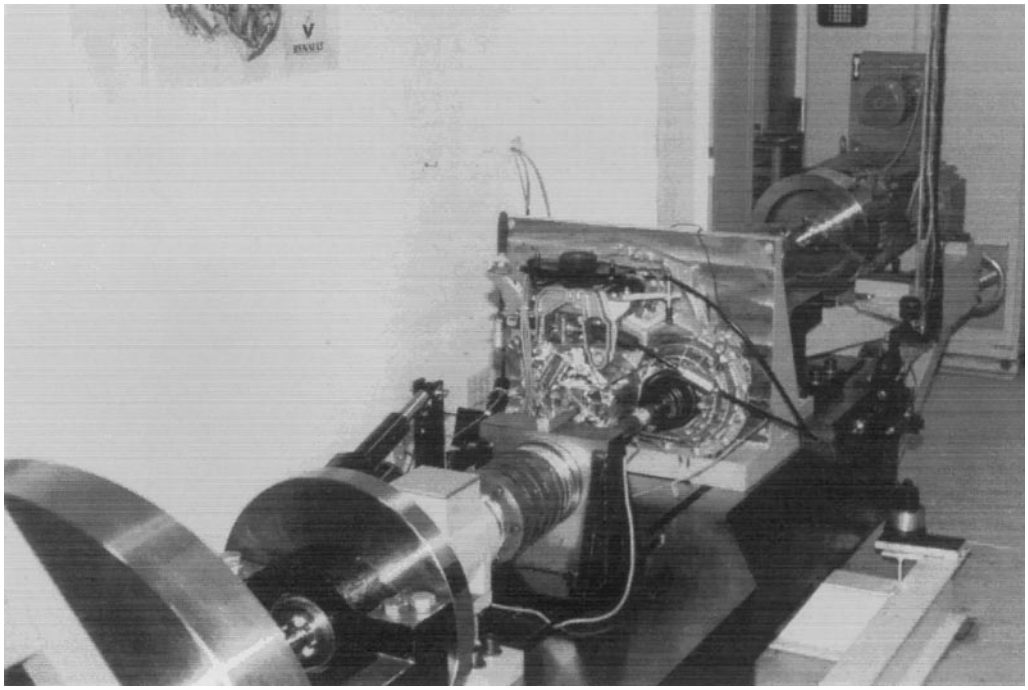

Figure 11. Experimental set-up.

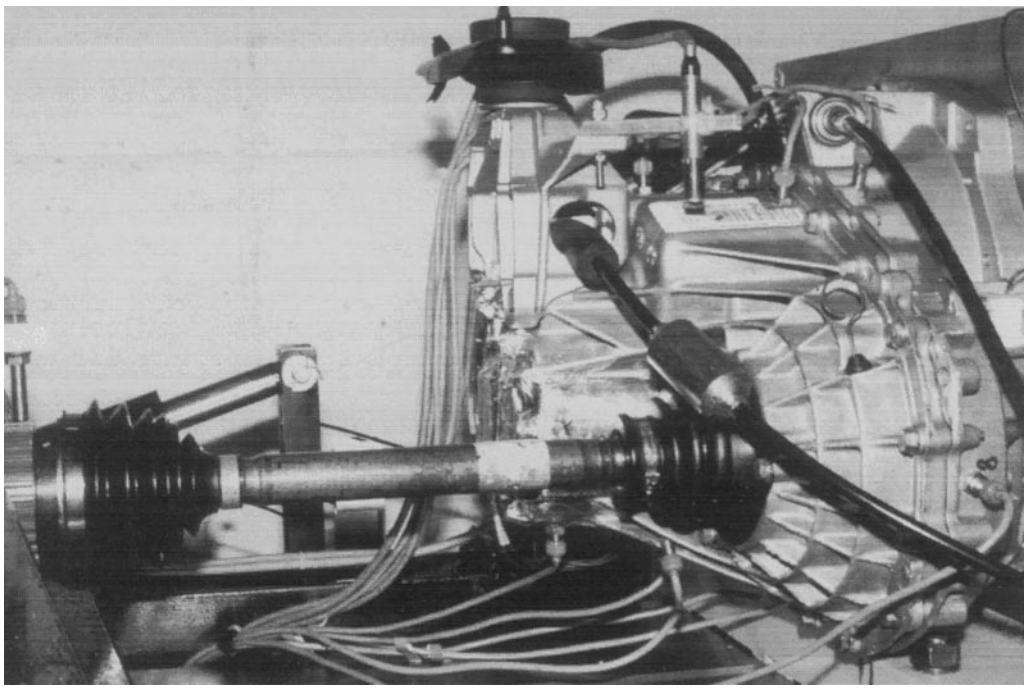

Figure 12. Instrumented gearbox and shaft.

time signal processing are carried out by using the LMS cada-X software. On-line processing is performed by order tracking. By using the above acquisition system, universal files are created for each test, allowing postprocessing and analysis with MATLAB. The instantaneous velocities and accelerations of meshing gear pairs in the transmission are obtained by demodulating signals from the inductive probes. The technique developed within the specific signal processing software is based upon frequency demodulation by means of the Hilbert transform combined with numerical filters. The instantaneous phase of the Hilbert transform of a sinusoidal carrier signal is proportional to the rotational angle of the gear under analysis, and the velocity time history is then obtained by differentiating the phase.

4.2. COMPARISON OF EXPERIMENTAL AND NUMERICAL RESULTS

The torsional model of the system consists of a branched system with four shafts and 200 elements. Identification of natural frequencies and mode shapes is achieved during a speed run-up with a constant mean torque allowing only one stage of the clutch to be active. Two tests are conducted to obtain, experimentally, two particular mode shapes of the driveline and the frequency responses corresponding to the harmonics of the engine speed of rotation are plotted in Figures 13 and 15.

4.2.1. *Natural frequency and modes shapes of the complete driveline*

The first measured and computed natural frequencies of the system are summarized in Table 1.

TABLE 1

Comparison of measured and computed natural frequencies

Mode number	Critical speed in r.p.m.	Experimental resonance frequency (F_m) in Hz	Computed resonance frequency (F_c) in Hz	Error $\lvert F_m - F_c \rvert / F_m$
1	–	–	2·7	–
2	540	18·0	18·5	2·8%
3	1810	60·3	58·4	3·1%
4	2050	68·3	64·2	5·9%

The first mode shape (2·7 Hz) corresponds to the so-called "surging" vibration mode occurring on the vehicle. This mode essentially involves torsional stiffnesses of the clutch and the drive axle shaft.

The second mode shape (18·0 Hz) involves displacement of drive axle shafts only.

The third mode shape (60·3 Hz) corresponds to a natural frequency of the drive system set-up and essentially involves Hooke's joint.

The fourth mode shape (68·3 Hz) is the so-called "gear rattle mode" which involves torsional high amplitudes of all meshing elements within the gearbox around the stiffnesses of the axle shafts and the clutch.

4.2.2. *Test conditions*

The first test (see Figure 13) was conducted with the fourth gear engaged with an angular value α of 16° and during a slow speed run-up from 300 to 700 r.p.m. The engine torque mean value is 100 Nm. During the run-up, the flywheel velocity data and four channels of data were recorded simultaneously. The second test (see Figure 15) was conducted with the fourth gear engaged with an angular value α of 7·5°. As previously, the same mean torque was applied and four channels of data were recorded.

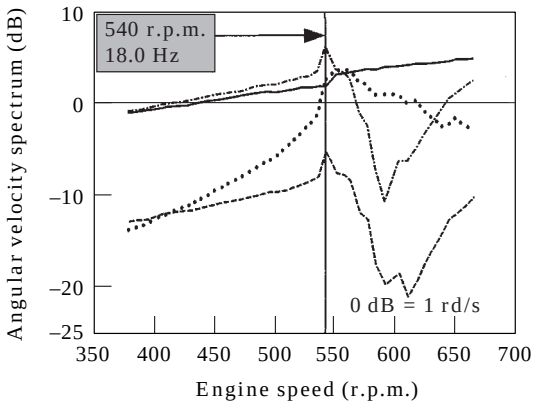

Figure 13. Measured forced response: identification of second mode shape (experiment). ——, Flywheel (reference signal); –·–·–, first pinion on input shaft; – – –, differential crown; · · · ·, transmission axle shaft.

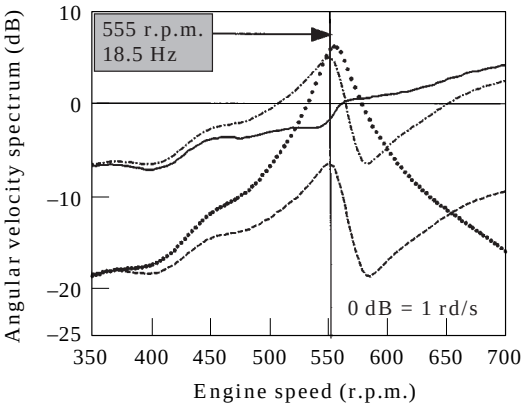

Figure 14. Computed forced response: identification of second mode shape (computation). Key as Figure 13.

4.2.3. *Comparing experimental and numerical results in the frequency domain*

In the simulation, multiple harmonics of the periodic torsional excitation were superimposed on the flywheel. F1, F2 and F4 harmonics were used in computing the forced response of the sytem. Equations of the system were linearized around the operating point corresponding to the test conditions. They were derived from the following assumptions: only the second stage of the clutch was active and the gear teeth remained in contact on the driving side. The response of the system was appropriately totalled from the forced responses for each harmonic. The direct method was used to solve the differential equations written on the modal basis. The tests were conducted by using order tracking analysis on the second harmonic of the engine speed of rotation. Computed and measured results are compared in the frequency domain by plotting angular velocity. Damping factors were deducted from the experimental results.

The measured and computed forced response curves for the first test are presented in Figures 13 and 14. The angular velocity amplitude of the flywheel, the input shaft, the differential crown and the drive axle shaft are displayed as a function of the mean engine speed of rotation in r.p.m. We observed experimentally a peak near the critical speed of 540 r.p.m. corresponding to a resonance frequency of 18·0 Hz (F2). A significant relative instantaneous angular velocity between the differential crown and the toothed wheel on the drive axle shaft was observed. As predicted, the corresponding mode shape involves torsional stiffness of the axle drive shaft.

For the second test, angular velocities of the flywheel, the 4/5th drive pinion on the input shaft and the corresponding fourth and fifth driven pinions on the long and short countershafts were plotted by order tracking. The frequency response in Figure 15 shows two peaks of magnitude and an amplification of gear motion with respect to the reference signal of the flywheel velocity. This test emphasizes the fourth mode (68·3 Hz) which involves high amplitudes of all the elements of the gearbox and causes rattle phenomena. The third mode (60·3 Hz) is close to

the fourth: it involves a strain mode of the Hooke's joint, thus, amplifying gear motion. By comparing experimental to computed results (see Figures 15 and 16), we notice that the progressions of the qualitative curves are in good agreement, and that the predicted linear behaviour of the system is close to the real behaviour of the transmission.

5. APPLICATIONS TO RECENT CARS

Transient dynamic response is required to simulate the phenomena in which non-linear effects, such as, clutch spring rate and damping, gear teeth backlash and so on cannot be neglected. In this section, measurements carried out on two recent cars during transient tests are compared to the predicted numerical results.

5.1. FIRST APPLICATION: SURGING ON THE RENAULT MEGANE VEHICLE

5.1.1. *Test conditions*

For this application, surging measurements were conducted on the Renault Megane vehicle. The test condition was in second gear from a constant engine speed of rotation of approximately 2000 r.p.m. As shown in Figure 17(a), surging is defined by the open throttle acceleration corresponding to an increase in the engine torque for 0·1 s. The test vehicle was instrumented by probes and two basic signals were measured: i.e., flywheel velocity and casing longitudinal acceleration (see Figures 17(b) and (c)).

5.1.2. *Driveline simulation model*

The transmission is composed of only two shafts and the torsional model of the driveline consisted of 67 elements. The axle drive shafts do not have the same length. Hooke's joint stiffness values are deduced from the measured stiffness between the wheels and the differential crown. A non-linear multi-staged clutch element is included in the model with both stiffness and hysteresis characteristics.

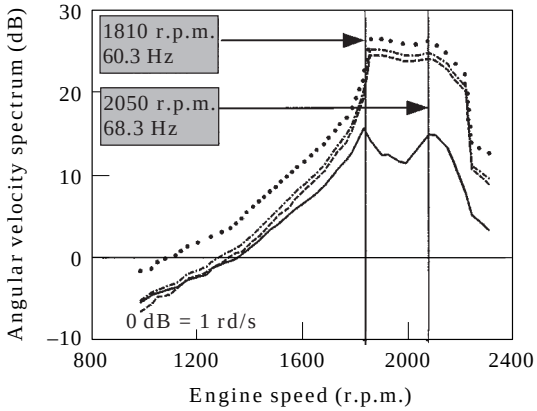

Figure 15. Measured forced response: identification of "gear rattle mode" (experiment). ——, Flywheel (reference signal); –·–·, 4/5th pinion on input shaft; ––, fourth idle pinion on countershaft; · · · ·, fifth idle pinion on countershaft.

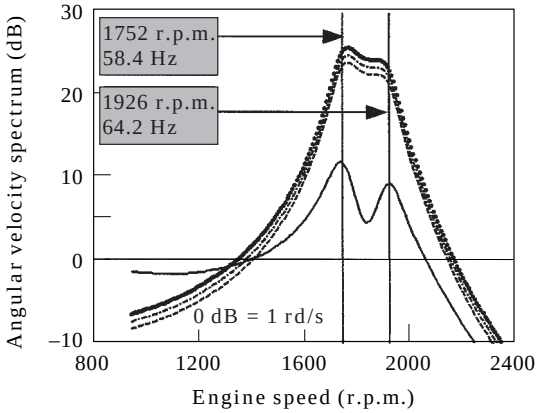

Figure 16. Computed forced response: identification of "gear rattle mode" (computation). Key as Figure 15.

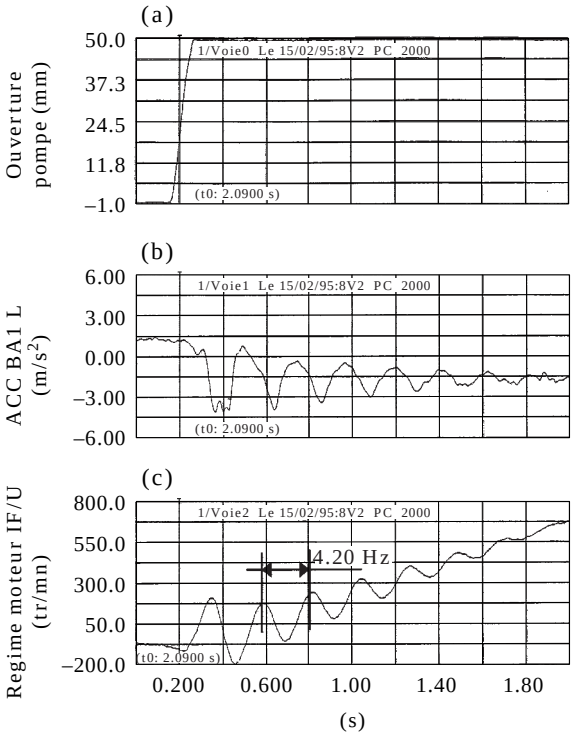

Figure 17. Surging: measured time responses.

The different stages of the clutch are used during surging. For the analysis, a damping modal value of 6% is introduced.

5.1.3. *Comparison of computer simulation and experimental results*

The simulation and experimental results plotted in Figures 17 and 18 are in good agreement. The resonance frequency predicted by computer simulation (4·34 Hz) is close to the experimental value (4·20 Hz). Plots of the casing acceleration and

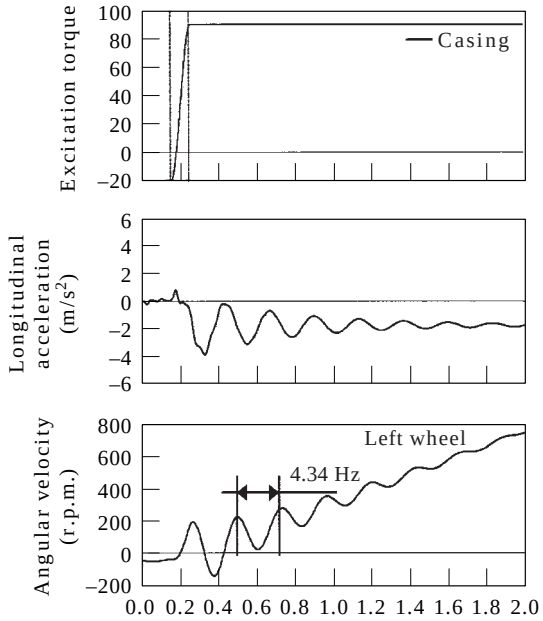

Figure 18. Surging: computed time responses.

the instantaneous angular velocity of the flywheel exhibit high amplitude damped oscillations at lower frequencies: i.e., during surging, the first mode of the driveline is involved.

5.2. SECOND APPLICATION: ACCELERATION/BACK-OUT/CLUTCH DISENGAGING ON THE RENAULT MASTER VEHICLE [23]

5.2.1. *Test conditions*

In this case, the test was conducted on the Renault Master vehicle. The test condition was a transient test in first gear including three steps: acceleration, back-out and clutch disengaging. Rotational gear velocities of the input shaft and the differential crown were measured during the test and the experimental results are presented in Figure 21 in which the three steps of the transient test can be clearly identified. After a run-up to the operating speed of 3700 r.p.m. (first step), the engine torque is suddenly decreased: the vehicle was no longer driven by the

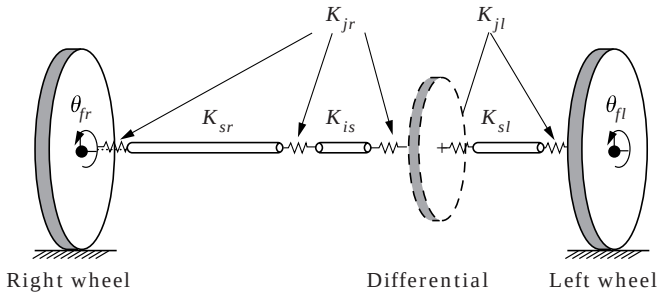

Figure 19. Axle drive shafts model.

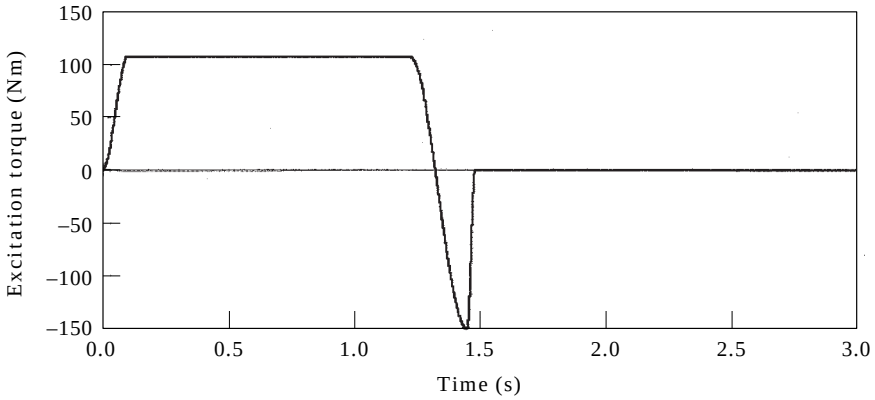

Figure 20. Excitation torque.

engine and the driveline was subjected to a resistive torque. This change from a positive torque to a negative torque resulted in velocity fluctuations of the input shaft (second step). During clutch disengagement (third step), the driveline was suddenly released and damped oscillations of the input shaft occurred.

5.2.2. *Driveline simulation model*

The torsional model of the driveline consisted of 76 elements and the transmission was modelled by using 65 elements. The left and right axle drive shafts were respectively composed of one and two shafts connected by Hooke's joints. They were modelled by rod elements connected to discrete stiffness elements (see Figure 19).

The torsional system was excited by a dynamic torque applied to the clutch disc. The excitation torque was defined by the time function shown in Figure 20: that is to say, for the first step, a torque value of 108 Nm was applied to obtain a rotational speed of 3700 r.p.m. in 2 s. For the second step, the engine torque was

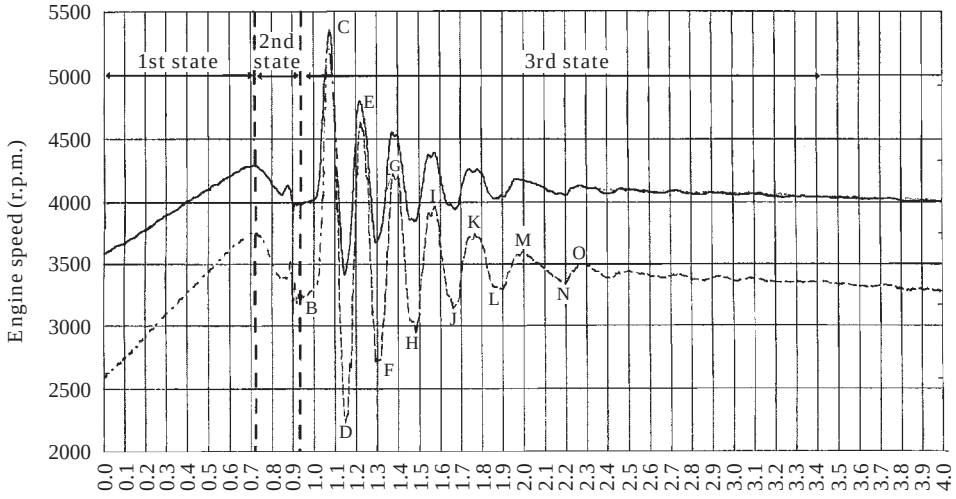

Figure 21. Measurements on Renault Master vehicle. –·–·, Third gear; ——, differential crown.

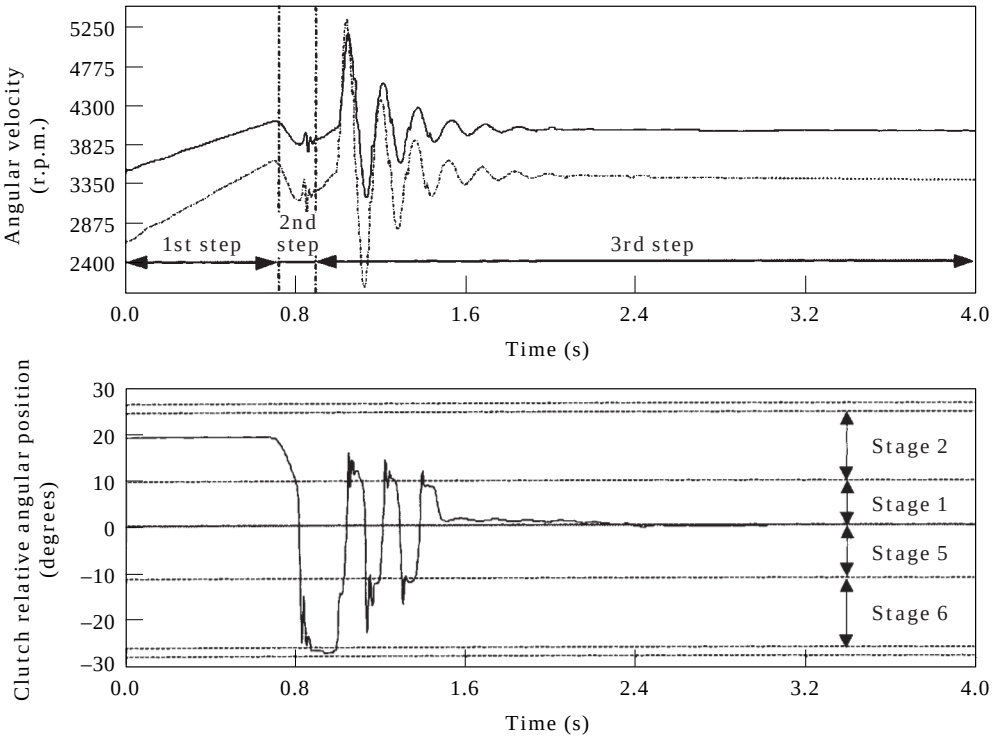

Figure 22. Computed time response. Key as Figure 21.

brought down to −150 Nm and the rotational speed was reduced to 3230 r.p.m. just before the third step. The torque was then suddenly reduced to zero in 0·03 s to simulate clutch disengagement.

5.2.3. *Comparison of computer simulation and experimental results*

The measured and predicted rotational velocity of the third gear and the differential crown are shown in Figures 21 and 22. Numerical simulation results are very close to the vehicle test measurements. Angular velocity plots exhibit the same following three steps. In the first step, the angular velocity of the third gear increases to the operating speed of 3700 r.p.m. In the second step, the angular velocity decreases because of the change of sign of the clutch torque. Stepping through the different stiffness stages involves oscillations. After clutch disengagement (third step), damped oscillations appeared due to the torque switching from a negative to a zero value. The model was up-dated by using the modal damping factors, and the results predicted by using computer simulation were shown to be relevant and in good agreement with the experimental time response.

6. CONCLUSIONS

This work includes the design of an experimental set-up and the development of computer software for predicting the dynamic behaviour of vehicle drivelines.

The experimental set-up shows the main torsional phenomena and validates the software results. Non-linear effects due to the multi-staged clutch with dry friction and gear backlashes have been given particular attention. Comparison between numerical and experimental results on two new cars have provided good agreement and show that the computer simulation can be very useful and efficient for the dynamic simulation of the driveline.

Furthermore, it will be very useful to simulate tests under conditions that are expensive and difficult to perform experimentally, and to reduce prototype development work. By using the simulation, the influence of the main design parameters can be evaluated and different design configurations can be compared in terms of strength, natural frequencies, frequency and transient responses. Continued developments in this direction will be of great benefit to the automotive industry by facilitating effective assessments of driveline torsional issues prior to production.

ACKNOWLEDGMENTS

The experimental results of this work have been achieved thanks to the financial aid provided by a contract with Renault; we would like to thank the management of Renault S.A. for sponsoring these studies. We would also like to thank them for their permission to publish the results on their test vehicles. We are grateful to A. Berlioz for his assistance and C. Develay for his contribution in conducting these experiments.

REFERENCES

1. R. J. Comparin and R. Singh 1990 *ASME Journal of Mechanical Design* **112**, 237–245. An analytical study of automotive neutral gear rattle.
2. C. Padmanabhan and R. Singh 1993 *Proceedings of Noise Control*, *Williamsburg*, *VA*, 607–612. Influence of clutch design on the reduction and perception of automotive transmission rattle noise.
3. C. Padmanabhan, R. C. Barlow, T. E. Rook and R. Singh 1995 *ASME Journal of Mechanical Design* **117**, 185–192. Computational issues associated with gear rattle analysis.
4. C. Padmanabhan, T. E. Rook and R. Singh 1995 *Proceedings of SAE Noise and Vibration Conference*, *Traverse City*, *MI* **951316**, 669–680. Modeling of automotive gear rattle phenomenon: state of the art.
5. Y. Chikatani and A. Suehiro 1991 *SAE Technical Paper Series* **911044**, 49–56. Reduction of idling rattle noise in trucks.
6. T. Sakai, Y. Doi, K. Yamamoto, T. Ogasawara and M. Narita 1981 *SAE Technical Paper Series* **810773**. Theoretical and experimental analysis of rattling noise of automotive gearbox.
7. R. Singh, H. Xie and R. J. Comparin 1989 *Journal of Sound and Vibration* **131**, 177–196. Analysis of automotive neutral gear rattle.
8. R. J. Comparin and R. Singh 1990 *Journal of Sound and Vibration* **142**, 101–124. Frequency response of a multi-degree of freedom system with clearances.
9. C. Padmanabhan and R. Singh 1995 *Journal of Sound and Vibration* **184**, 767–799. Vibration dynamics analysis of a piecewise non-linear system subject to dual harmonic excitation using parametric continuation.

10. R. L. Seaman, C. E. Johnson and R. F. Hamilton 1984 *SAE Technical Paper Series* **841686**. Component inertial effects on transmission design.
11. F. Pfeiffer and W. Prestl 1996 *Proceedings of I. Mech. E., VDI Berichte* **1230**, 719–737. Rattling in gears—a review.
12. M. D. Crocker, J. P. March and R. J. Greer 1990 *I. Mech. E C*404/005, *Conference on Gearbox Noise and Vibration*, *Cambridge*, *England*, 121–127. Transmission rattle analysis.
13. O. Johnson and N. Hirami 1991 *SAE Technical Paper Series* **911082**, 381–396. Diagnosis and objective evaluation of gear rattle.
14. T. Fujimoto, Y. Chikatani and J. Kojima 1987 *SAE Technical Paper Series* **870395**, 1–12. Reduction of idling rattle in manual transmission.
15. S. Ohnuma, S. Yahata, M. Inagawa and T. Fujimoto 1985 *SAE Technical Paper Series* **850979**, 159–167. Research on idling rattle of manual transmission.
16. T. Shimizu 1993 *Seventh Pacific Conference and Exposition on Automotive Engineering*, *Phoenix*, *AZ*, *SAE Technical Paper Series* **932003**, 7–13. Mechanism of the idle gear rattle synchronized with engine rotation.
17. A. Szadkowski 1991 *International Congress and Exposition Detroit Michigan SAE Technical Paper Series* **910641**, 81–97. Mathematical model and computer simulation of idle gear rattle.
18. Ph. Couderc 1997 *Thèse de Doctorat de l'INSA de Lyon*. Comportement dynamique des chaînes de transmission automobiles.
19. G. J. Fudala, T. C. Engle and A. V. Karvelis 1987 *SAE Technical Paper Series* **870396**. A system approach to reducing gear rattle.
20. A. Laschet 1994 *SAE Technical Paper Series* **941011**. Computer simulation of vibrations in vehicle powertrains considering nonlinear effects in clutches and manual transmissions.
21. M. Kamo, H. Yamamoto, H. Koga and K. Umezawa 1996 *SAE Technical Paper Series* **960726**, 221–227. Analysis method for the contribution rate of each pair of gears on the driveline gear rattle.
22. M. Lalanne and G. Ferraris 1997 *Rotordynamics prediction in engineering*. Chichester: John Wiley and Sons; second edition.
23. M. Carin and D. Derrien 1996 *Rueil-Malmaison*: *RENAULT/D.R./M.P.-Service* 00076, *Note de service*: *H*31/96.560. Comportement dynamique d'une transmission—comparaison entre mesures sur véhicule et simulation VICTOR.

APPENDIX: LIST OF SYMBOLS

T_c	clutch torque
k_{si}	stiffness of the clutch for the stage i
$\theta_1, \dot{\theta}_1$	angular displacement and velocity of the fly-wheel
$\theta_2, \dot{\theta}_2$	angular displacement and velocity of the clutch hub
β_i	torque value at the transition point for the stage i of the clutch
α_i	angular range of the clutch for stage i
P_d	preloaded torque for the direct edge of the clutch
P_r	preloaded torque for the rear edge of the clutch
σ	smoothing parameter
$[K_c]$	stiffness matrix of the clutch
$[C_c]$	viscous damping matrix of the clutch
$[\mathbf{C}_{ext}]$	external torque excitation vector applied on the clutch
T_{eng}	engine torque
T_g	gear torque
k_g	stiffness of two teeth in contact with a gear
c_g	viscous damping of two teeth in contact with a gear

R	primitive radius of a pinion
δ	relative displacement of a tooth of the drive gear in the backlash
b_g	backlash of a gear
$[K_{gi}]$	stiffness matrix of two teeth in contact with gear i
$[C_{gi}]$	viscous damping matrix of two teeth in contact with gear i
$\boldsymbol{\delta}_{ss}$	nodal displacement vector of the sub-system {vehicle, MPU, rear chassis, rear transmission}
$\theta_{fl}, \dot{\theta}_{fl}, \theta_{fr}, \dot{\theta}_{fr}$	angular displacement and velocity of, respectively, the left wheel and the right wheel
X, X_{fl}, X_{fr}	displacement of, respectively, the sub-system {vehicle, MPU, rear chassis, rear transmission}, the left wheel and the right wheel
$[M_{ss}]$	Mass matrix of the sub-system {vehicle, MPU, rear chassis, rear transmission}
$[K_{ss}]$	stiffness matrix of the sub-system {vehicle, MPU, rear chassis, rear transmission}
K_{rfc}, K_{lfc}	stiffness between the sub-system and respectively the right wheel and the left wheel
K_{sr}, K_{sl}	right and left axle shaft stiffness
K_{is}	intermediate shaft stiffness
K_{jr}, K_{jl}	right and left Hooke's joint stiffness
K_t	tire stiffness in the direction of vehicle motion